

# GEOLOGICAL FIELD TRIPS AND MAPS

2026  
Vol. 18 (1.1)

Jurassic volcanism in the western Tethys  
(Iberian Range, Spain): geological maps

<https://doi.org/10.3301/GFT.2026.01>



SOCIETÀ GEOLOGICA ITALIANA ETS  
FONDATA NEL 1881 - ENTE MORALE R. D. 17 OTTOBRE 1885

 **ISPR**  
Istituto Superiore per la Protezione  
e la Ricerca Ambientale



# Geological Field Trips and Maps



Periodico semestrale del Servizio Geologico d'Italia - ISPRA e della Società Geologica Italiana ETS  
 Geol. F. Trips Maps, Vol. 18 No.1.1 (2026), 18 pp., 6 figs. (<https://doi.org/10.3301/GFT.2026.01>)

## Jurassic volcanism in the western Tethys (Iberian Range, Spain): geological maps

José Emilio Cortés<sup>1</sup>

<sup>1</sup> Departamento de Geodinámica, Estratigrafía y Paleontología, Facultad de Ciencias Geológicas, Universidad Complutense de Madrid, José Antonio Novais 12, 28040 Madrid, Spain.

JEC, [0000-0003-0477-6837](#).

Corresponding author e-mail address: [jocortes@ucm.es](mailto:jocortes@ucm.es)

### Responsible Director

*Maria Siclari (ad interim)* (ISPRA-Roma)

### Editor in Chief

*Marco Malusà* (Università Milano-Bicocca)

### Editorial Manager

*Angelo Cipriani* (ISPRA-Roma) - *Silvana Falcetti* (ISPRA-Roma)

*Fabio Massimo Petti* (Società Geologica Italiana - Roma) - *Matteo Simonetti* (ISPRA - Roma) - *Alessandro Zuccari* (Società Geologica Italiana - Roma)

### Associate Editors

*M. Caggiati* (University of Padova), *M. Della Seta* (Sapienza University of Rome), *L. Disperati* (University of Siena),  
*J.-L. Epard* (University of Lausanne), *S. Fabbi* (Sapienza University of Rome), *V. Galluzzi* (INAF IAPS Roma),  
*G. Giordano* (University Roma Tre), *G. Griesmeier* (GeoSphere Austria), *P.J. Haproff* (University of North Carolina Wilmington),  
*D. Pieruccioni* (ISPRA-Rome), *R. Maniscalco* (University of Catania), *C. Muraro* (ISPRA-Rome),  
*A. Plunder* (BRGM - French Geological Survey), *G. Toscani* (University of Pavia), *S. Zanchetta* (University of Milano-Bicocca)

### Editorial Advisory Board

*D. Bernoulli*, *F. Calamita*, *W. Cavazza*, *F.L. Chiocci*, *R. Compagnoni*, *D. Cosentino*, *S. Critelli*, *G.V. Dal Piaz*, *P. Di Stefano*, *C. Doglioni*,  
*E. Erba*, *R. Fantoni*, *M. Marino*, *M. Mellini*, *S. Milli*, *E. Chiarini*, *V. Pascucci*, *L. Passeri*, *A. Peccerillo*, *P. Ronchi*, *L. Simone*, *I. Spalla*,  
*L.H. Tanner*, *C. Venturini*, *G. Zuffa*.

### Technical Advisory Board for Geological Maps

*R. Bonomo* (ISPRA-Rome), *F. Capotorti* (ISPRA-Rome), *P. Cipollari* (University of Roma Tre), *E. De Beni* (INGV, Osservatorio Etneo),  
*C. Di Celma* (University of Camerino), *A. Ellero* (CNR-IGG Pisa), *F. Gianotti* (University of Torino), *S. Grossi* (ISPRA-Rome),  
*F. Lucchi* (University of Bologna), *M. Nocentini* (ISPRA-Rome), *S. Orefice* (ISPRA-Rome), *F. Papasodaro* (ISPRA-Rome),  
*G. Radeff* (ISPRA-Rome), *F. Remitti* (University of Modena), *G. Romagnoli* (ISPRA-Rome), *L. Sabato* (University of Bari),  
*F. Stendardi* (University of Pavia), *M. Zucali* (University of Milano), *M. Tropeano* (University of Bari),  
*G. Vignaroli* (University of Bologna), *L. Vita* (ISPRA-Rome), *M. Zucchi* (University of Bari)

© 2026. The Author(s).

This is an open access article under the terms of the [Creative Commons Attribution License](#), which permits use, distribution and reproduction in any medium, provided the original work is properly cited.

### Cover

*Above:* Volcanic level V<sub>9</sub> in the CAMARENA DE LA SIERRA.5 outcrop.

*Below:* *Spinammatoceras* sp. (Aalenian, *bradfordensis* Zone) from the CAMARENA DE LA SIERRA.2 outcrop.

ISSN: 2038-4947 [online]

<http://gftm.socgeol.it/>

The Geological Survey of Italy, the Società Geologica Italiana and the Editorial group are not responsible for the ideas, opinions and contents of the guides published; the Authors of each paper are responsible for the ideas, opinions and contents published.

Il Servizio Geologico d'Italia, la Società Geologica Italiana e il Gruppo editoriale non sono responsabili delle opinioni espresse e delle affermazioni pubblicate nella guida; l'Autore/i è/sono il/i solo/i responsabile/i.

**INDEX**

|   |    |
|---|----|
| <b>Introduction</b> .....   | 4  |
| <b>Palaeogeography, lithostratigraphy, chronostratigraphy, volcanism, and tectonics</b> ..... | 4  |
| Geological and palaeogeographical setting .....   | 4  |
| Lithostratigraphy and sedimentary cycles .....  | 6  |
| Quantifying and dating the volcanic levels .....  | 9  |
| Nature and age of the volcanism .....   | 9  |
| Volcanism during the first Mesozoic post-rifting stage of the Iberian Basin .....             | 13 |
| <b>Methods and techniques</b> .....   | 13 |
| Fieldwork .....   | 13 |
| Field mapping digitising process .....  | 13 |
| <b>Contents description</b> .....   | 14 |
| Criteria used to name the volcanic outcrops .....   | 14 |
| Maps number, dimensions, and content .....  | 14 |
| <b>Discussion and conclusions</b> .....   | 15 |
| <b>References</b> .....   | 17 |

## ABSTRACT

Occurrences of interbedded volcanic deposits in the Jurassic marine carbonate successions of the SE Spanish Iberian Range (Iberian Plate) have been reported since the 1930s. However, it was not until now, almost 85 years later, that these volcanic deposits have been quantified and dated. Eight sites containing single or multiple volcanic rock outcrops are detected, where 13 successive volcanic levels are differentiated using biostratigraphic methods. The results indicate that the volcanic manifestations were distributed throughout the early Pliensbachian–early Bajocian interval. The starting point for this quantification and dating was the geological mapping of the volcanic outcrops and surrounding sedimentary formations. The geological mapping was carried out in the field using traditional methods, such as enlargements of maps on paper at a scale of 1:25,000 provided by the Instituto Geográfico Nacional (IGN) and at a scale of 1:10,000 by the Institut Cartogràfic Valencià. The hand-drawn geological features were later digitized using several software programs (AutoCAD, ArcGIS, Adobe Illustrator, and Adobe Photoshop) and presented in portable document format (.pdf) in this work. Georeferenced sheets of the National Topographic Base of Spain (1:25,000) in digital (.dwg) format were used as the topographic base of the maps. Orthoimages and Digital Elevation Models were also deployed. All the material (vector topographic base, orthoimages, and DEMs) was provided by the Instituto Geográfico Nacional of Spain. The final maps represent a complete location of all known Jurassic volcanic manifestations in the Iberian Range, which may be useful in further multidisciplinary geological work.

**Keywords:** geological maps, Jurassic, Iberian Range, intraplate volcanism, biostratigraphic dating.

## INTRODUCTION

The existence of volcanic rocks in the SE of the Iberian Range dates from the mid-1930s (Bakx, 1935; Martin, 1936), occurring as mostly volcanoclastic levels interbedded between the Lower and Middle Jurassic marine carbonate successions of the Javalambre and Camarena regions (Teruel province). Later works revealed the presence of some of these levels in other new specific geographical locations at the confluence of the provinces of Teruel, Castellón, and Valencia (e.g., Gautier, 1968; Ortí & Sanfeliu, 1971; Gómez et al., 1976).

Up to that time, all reports consisted of isolated and disconnected descriptions of findings of scattered volcanic manifestations. Nevertheless, more and more outcrops were gradually becoming known in a broad region.

Crucial was the work of Gómez (1979), where several zones of structural discontinuity were identified (the Caudiel and Alcublas fault zones with NW–SE direction and the NE–SW or NNE–SSW trending Teruel Fault Zone), along which the outcrops of volcanic rocks are aligned (Fig. 1).

In the early 1980s, Ortí & Vaquer (1980) tried a spatio-temporal integration of all the outcrops known at that time. Unfortunately, the volcanic levels were correlated only

based on their position within the lithostratigraphic units defined by Goy et al. (1976), which frequently have very diachronic boundaries.

Attempts were made to date certain volcanic levels using radiometric methods (Gautier & Odin, 1985; Odin et al., 1988). However, the ages obtained were much more modern than the sediments. The fact that the Jurassic successions containing volcanic manifestations are especially rich in ammonites and brachiopods provided, *a priori*, a promising way to undertake the task of quantifying, dating, and correlating the volcanic levels using biostratigraphic methods. A research project, which began in the early 2000s and led to the author's PhD, was focused on the attainment of three main goals: 1) quantification of magmatic manifestations and biostratigraphical dating of each volcanic level placed within the Lower and Middle Jurassic sedimentary successions, 2) finding the time interval of the volcanism represented by primary volcanic deposits, and 3) determining the depositional architecture of the lithostratigraphic units that contain these volcanic deposits.

For these purposes, biostratigraphic, sedimentological, and cyclostratigraphic analyses were performed. The criteria for distinguishing between the age of the volcanic stratigraphic placement and the actual age of the volcanic emissions were also reviewed and implemented.

A set of sites with interbedded volcanic levels was identified (Fig. 1), the first phase of the project planning being their geological mapping. Despite the availability of geological maps at a scale of 1:50,000, published by the Instituto Geológico y Minero de España (IGME) between 1974 and 1983 (Gautier, 1974; Abril et al., 1975, 1978; Campos et al., 1977; Lazuen & Roldán, 1977; Adrover et al., 1983), a new mapping at a more detailed scale was deemed necessary, covering each outcrop of volcanic rocks and surrounding carbonate sediments.

## PALAEOGEOGRAPHY, LITHOSTRATIGRAPHY, CHRONOSTRATIGRAPHY, VOLCANISM, AND TECTONICS

### Geological and palaeogeographical setting

The development of a series of Permo-Triassic rift systems, whose geometry was determined by the configuration of ancient inherited Variscan structures, marked the beginning of the Alpine Cycle in Iberia. Following the Triassic Period, Iberia underwent two main kinematic phases. A first extensional phase related to rifting and the opening of the Central and North Atlantic (Vergés et al., 2019) and the Alpine-Ligurian Tethys (Schettino & Turco, 2011) during the Jurassic (Fig. 2), followed by a second compressional phase originated by the convergence of Africa and Europe from the Cretaceous to the present (Vergés et al., 2019).

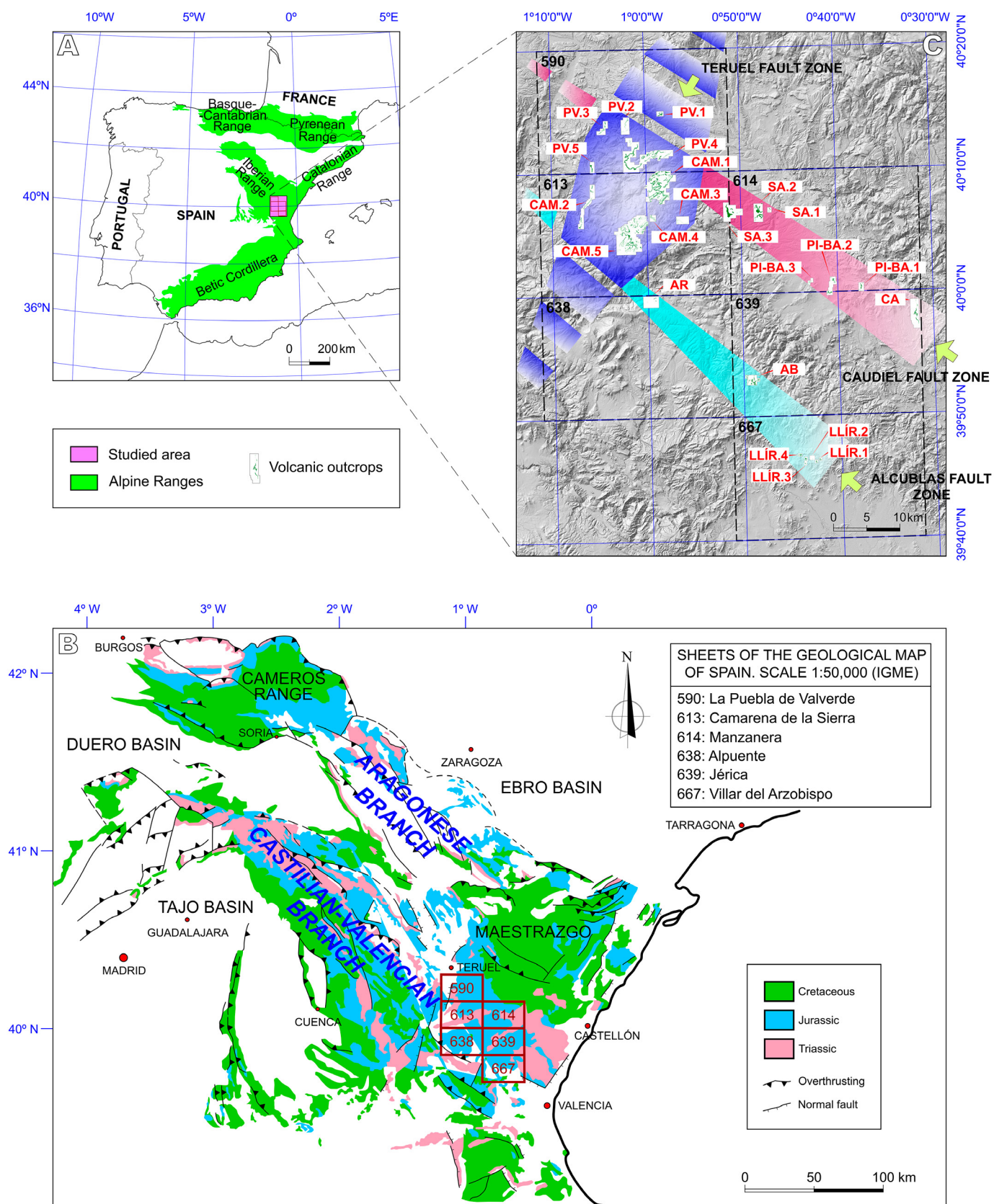


**Fig. 1 - A)** Location of the Alpine ranges in the Iberian Peninsula and the studied area in the Iberian Range. **B)** Geological location of the six sheets of the Geological Map of Spain at the scale of 1:50,000 that include the studied area. **C)** Location of the volcanic outcrops along the Caudiel, Alcublas, and Teruel fault zones within the six sheets of the Geological Map of Spain (scale 1:50,000) in the studied area. Outcrops abbreviations: CA (Caudiel), PI-BA.1, 2, and 3 (Pina-Barracas.1, 2, and 3), SA.1, 2, and 3 (Sarrión.1, 2, and 3), LLÍR.1, 2, 3, and 4 (Llíria.1, 2, 3, and 4), AB (Abejuela), AR (Arcos de las Salinas), PV.1, 2, 3, 4, and 5 (La Puebla de Valverde.1, 2, 3, 4, and 5), CAM.1, 2, 3, 4, and 5 (Camarena de la Sierra.1, 2, 3, 4, and 5).

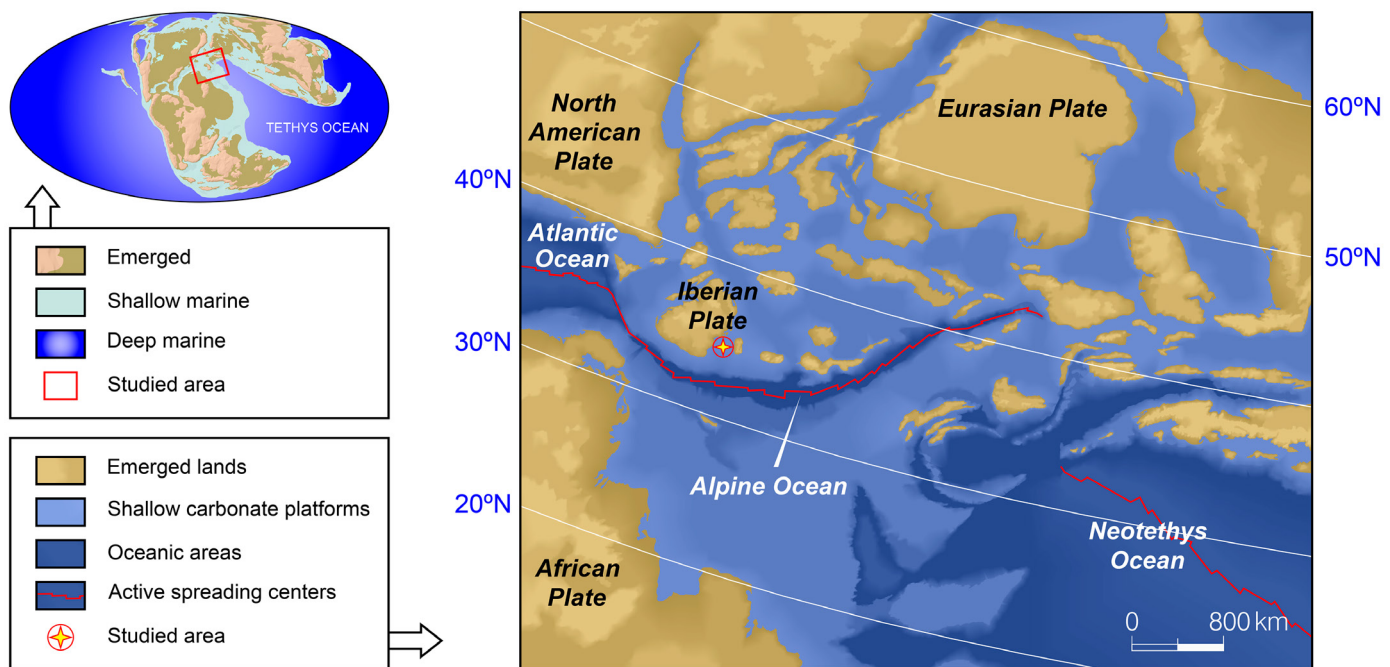


Fig. 2 - Palaeogeographic reconstruction of the western Tethys during the Early-Middle Jurassic. Modified from Schettino & Turco (2011) and Blakey (2011). Palaeolatitudes adapted from Osete et al. (2011).

Iberia became an individualized plate as its margins were gradually shaped over time through the first extensional phase, constituting both the western boundary of the Tethys Ocean and the eastern boundary of the proto-Atlantic Ocean (Gómez et al., 2019). In the Iberian Plate, several pre-orogenic basins (e.g., Basque-Cantabrian, Pyrenean, Catalonian coastal, Iberian, and Betic basins) were formed, bordering the uplifted and emerged Iberian Massif. The Iberian Basin should be considered a system of shallow carbonate platforms located at the eastern palaeomargin of the Iberian Plate (Gómez et al., 2004) at latitudes of about 30-35°N during the Early and Middle Jurassic (Osete et al., 2011). In this palaeogeographic scenario, volcanic deposits accumulated in the SE of the Iberian carbonate platforms system (Fig. 2).

Throughout the first extensional pre-orogenic phase of the Alpine Cycle, the Iberian carbonate platforms system was affected by two rifting periods, each followed by one post-rifting stage. The first rifting period started in the early Permian (Sakmarian) and ended in the Late Triassic (latest Norian). The first post-rifting stage began at the Late Triassic (Rhaetian) and extended to the Middle-Late Jurassic boundary (Gómez et al., 2004, 2019). The second rifting period developed from the boundary between the Middle and the Late Jurassic (Callovian–Oxfordian) up to the Early Cretaceous (late Albian). The second post-rifting stage extended from the end of the rifting period to the Cretaceous–Paleogene boundary (Gómez et al., 2019).

The Iberian platforms system evolved to a folded range (Iberian Range) as a result of the Cenozoic compressional

phase. The Iberian Range is an NW–SE trending moderately deformed intraplate fold-and-thrust chain with a low degree of shortening. Within it, several areas can be distinguished: the NW Cameros area, the Aragonese Branch, the Castilian-Valencian Branch (both branches constituting the central and eastern part of the Iberian Range), and the El Maestrazgo area, which works as the link between the Iberian and the Catalonian Coastal mountain ridges (Gómez et al., 2019).

The sediments and volcanics studied are spatially located in the southeastern part of the Iberian Range (where its Castilian-Valencian and Aragonese branches converge) (Fig. 1) and were temporally included in the first post-rifting stage of the Iberian Basin geodynamic evolution.

### Lithostratigraphy and sedimentary cycles

The volcanic levels are interbedded in the Cuevas Labradas (upper part), Barahona, Turmiel, Casinos, and the lower part of the El Pedregal formations (Cortés, 2018, 2020a, 2020b, 2021) (Fig. 3). However, other Jurassic lithostratigraphic units have been mapped and included in the geological maps. Such units are the Cortes de Tajuña, Cerro del Pez, Moscardón, Domeño, Yátova, Sot de Chera, Loriguilla, Higuueruelas, and Villar del Arzobispo formations, as well as the Arroyofrío Bed.

The Cortes de Tajuña Formation consists of ochreous carniolas, crystalline dolostones, and carbonate breccias, massive or poorly stratified in very thick and discontinuous banks. Its age spans from the Upper Triassic (Rhaetian) to

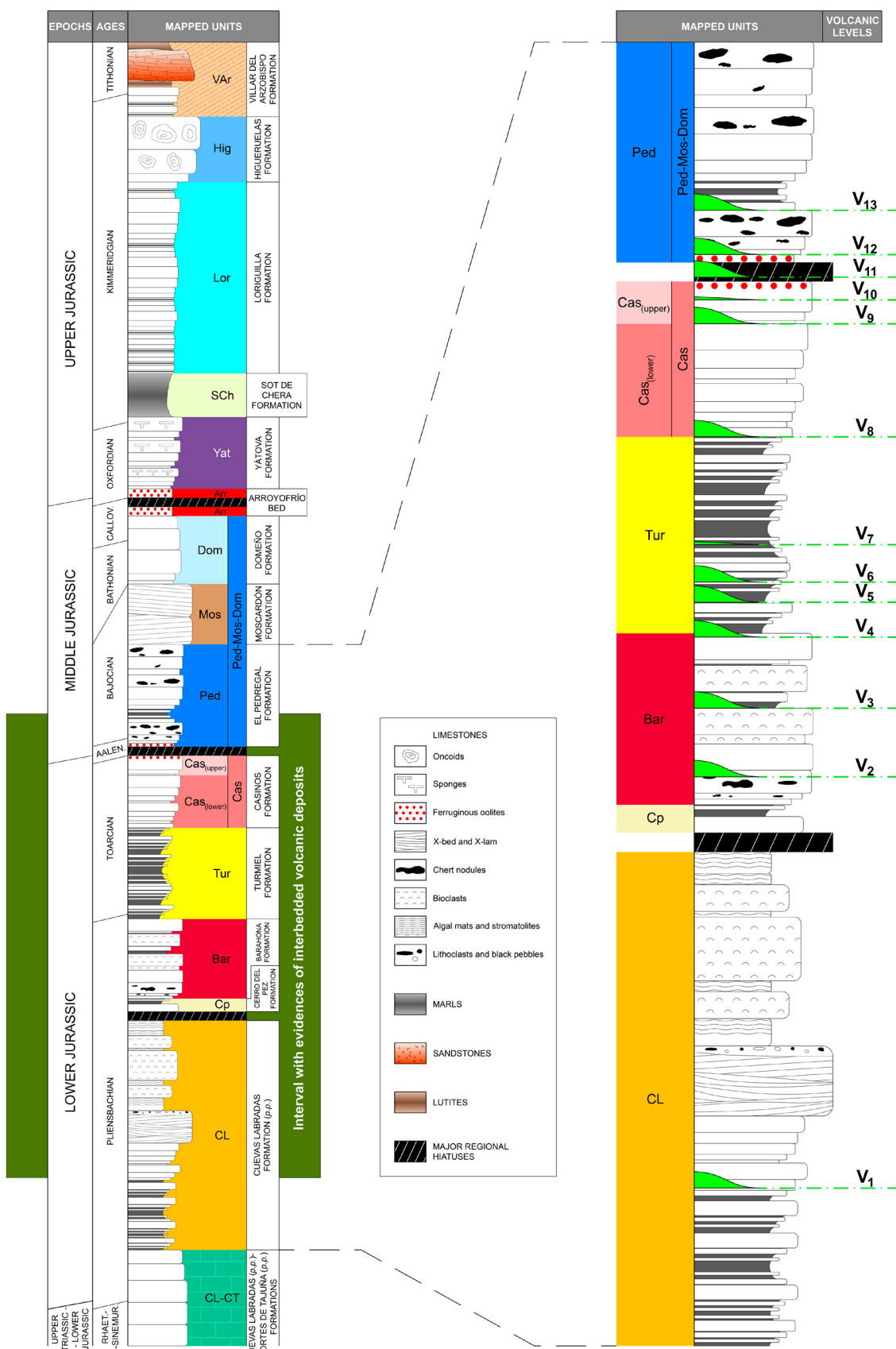


Fig. 3 - Synthetic stratigraphic section showing the Jurassic mapped units, lithologies, main regional hiatuses, and the interval with evidence of interbedded volcanic deposits (on the left). Enlargement of the part of the synthetic stratigraphic section containing the volcanic levels to point out their stratigraphic position (on the right). The respective ages of the 13 volcanic levels are available in the text.

the Lower Jurassic (Sinemurian) (Goy et al., 1976; Gómez et al., 2004).

The Cuevas Labradas Formation is constituted by mudstones, bioclastic wackestones to packstones, cross-bedded grainstones, crystalline dolostones, and bindstones (algal mats and stromatolites). Yellow marls containing bivalves, crinoids, and scarce ammonoids are also present, matching peaks of maximum deepening in some depositional sequences. During lowstand stages, mudstones, bindstones, mottled (greenish-yellow, whitish, or blackish) clays, and calcareous breccias are dominant, showing features of subaerial expositions. Facies associations reflect from relatively open marine, to subtidal, restricted lagoon, low- and high-energy intertidal, and supratidal environments. The age interval ranges from the late Sinemurian to the early Pliensbachian (*davoei* Zone) up to the late Pliensbachian (*margaritatus* Zone) locally (Goy et al., 1976).

The Cerro del Pez Formation is an alternation of grey marls and bioclastic mudstone to wackestone limestones. The top of the parasequences may feature hardgrounds, ferruginous crusts, and bioturbation. Sedimentation occurred on a low-energy platform below the base level of the waves, although it was occasionally subjected to storm action. The platform was connected to the open sea, allowing frequent entry of ammonite shells. Brachiopods are also abundant. Its age ranges from the *davoei* to the *margaritatus* zones (Goy et al., 1976). This formation often is absent or quite reduced in thickness along the studied area (Gómez, 1979; Cortés, 2018).

The Barahona Formation comprises bioclastic wackestones to packstones, sometimes grainstones, and marly interbeds in its lower part, which can be absent. Chert nodules and hardgrounds capping some parasequences are common. Sedimentation occurred on relatively shallow subtidal platforms, usually located below the fair-weather wave base and influenced by storm activity, which were colonised by benthic organisms (mainly crinoids, oysters, and scarce brachiopods). Tractional structures are not unusual when bioclastic shoals emerged. The Barahona Formation ranges in age from the late Pliensbachian (*margaritatus* Zone p.p.) to the early Toarcian (*tenuicostatum* Zone p.p.) (Goy et al., 1976).

The Turmiel Formation consists of an alternation of marls and mudstones to packstones, which was deposited on low-energy, external, and open marine carbonate platforms generally situated below the storm wave base. Lithology, facies associations, and diversity of benthic fauna (echinoids, bivalves, bryozoans, brachiopods, and ammonites) indicate widespread deepening of the Iberian carbonate platform system. The Turmiel Formation is Toarcian in age (*tenuicostatum* Zone–*bifrons* Zone), the lower part can be late Pliensbachian (*spinatum* Zone), and the upper part can locally reach the early Aalenian (*opalinum* Zone) (Goy et al., 1976).

The Casinos Formation is characterised by bluish-grey nodular mudstones and bioclastic wackestones with thin marly beds often occurring in its lower part. The upper part, constituted by yellowish-brown nodular and bioclastic wackestones–packstones, can be locally and regionally absent (Cortés, 2018). Facies associations and organisms (crinoids, inoceramids, oysters, brachiopods, gastropods, belemnites, and necroplanktic drifted ammonoid shells) are indicators of external, shallow, and open carbonate platform settings. In the uppermost part, the formation sometimes shows ferruginous or phosphatic oolites and episodes of regional emersion. The Casinos Formation extends from the early Toarcian (*bifrons* Zone) to the Aalenian (*murchisonae* Zone p.p.) (Gómez & Goy, 1979; Gómez et al., 2003).

The El Pedregal Formation contains mudstones and bioclastic wackestones to packstones with bivalves (microfilaments), echinoderms, oysters, sponges, brachiopods, belemnites, and ammonites. They can locally show interlayered marly beds, with chert nodules common in limestones. At the base of the formation, limestones containing ferruginous or phosphatic oolites can be found. The El Pedregal Formation develops in external and shallow carbonate platform environments affected by storms. The unit begins at the upper part of the Aalenian *murchisonae* Zone. The top of the unit corresponds to the late Bajocian (*niortense* and *garantiana* zones) (Gómez & Fernández-López, 2004, 2006).

The Moscardón Formation consists mainly of bioclastic packstones to grainstones arranged in beds several metres thick. This formation contains abundant macrofossils, such as ammonites, belemnites, brachiopods, sponges, echinoderms, bryozoans, and bivalves, indicative of open marine environments. However, planar and festoon cross-lamination, ripples, and bioclastic rills are common, indicating high-energy and very shallow conditions. The oldest sediments of this unit correspond to the Bajocian *garantiana* Zone, although they may also be from the early Bathonian (*zigzag* Zone). In contrast, the upper part of the unit varies in age from the late Bajocian (*parkinsoni* Zone) to the early Bathonian (*zigzag* Zone) (Gómez & Fernández-López, 2004, 2006).

The Domeño Formation is usually composed of wackestones of microfilaments, interbedded with marly limestones. Chert nodules can be abundant, and open-marine bivalves, brachiopods, echinoderms, ammonites, and belemnites are common. The sediments of this formation were deposited on an open-marine, external carbonate platform. The base of the Domeño Formation is diachronous, varying in age from the Bathonian *zigzag* Zone up to the Bathonian *progracilis* Zone. The top is marked by the presence of the iron-oolitic Arroyofrío Bed, which is also diachronous. (Gómez & Fernández-López, 2004, 2006).

The Arroyofrío Bed consists of reddish wackestone to packstone limestones with abundant ferruginous oolites, ferruginous crusts, and ferruginous cement. They contain macrofauna, mainly of belemnites, ammonites, and sponges. The thickness of the Arroyofrío Bed varies greatly, from a few centimetres to 2–3 metres. Ammonites indicative of the early and middle Callovian, and middle and late Oxfordian were recognised. The late Callovian and early Oxfordian represent a stratigraphic gap within this bed. This unit has been interpreted as resedimentations from lateritic soils or as formed in coastal to shallow marine domains (Gómez & Goy, 1979; Aurell et al., 2019).

The Yátova Formation consists of grey open marine wackestone to packstone limestones with a nodular appearance, rich in siliceous sponges, ammonites, brachiopods, crinoids, bivalves, belemnites, echinoids, and serpulids. Its upper boundary is a net contact showing a concentration of fauna and ferruginous crusts. Its age ranges from the middle Oxfordian *transversarium* Zone to the late Oxfordian *hypselum* Zone (Gómez & Goy, 1979; Aurell et al., 2019).

The Sot de Chera Formation consists of open-ramp grey, yellow, or beige marls and thin nodular limestones. Its age is Kimmeridgian *p.p.* (Aurell et al., 2019).

The Loriguilla Formation is a well-bedded alternation of open-ramp thin slabby calcareous marls (or marls) and thicker grey mudstone limestones. As a whole, the unit displays a predominantly calcareous rhythmic character. Its age is early Kimmeridgian (Gómez & Goy, 1979; Aurell et al., 2019).

The Higueruelas Formation consists of mid-ramp, thick-bedded oolitic, oncolitic, biohermal, and bioclastic limestones, late Kimmeridgian in age (Gómez & Goy, 1979; Aurell et al., 2019).

The Villar del Arzobispo Formation consists of coastal siliciclastic sediments, including red mudstones with intercalations of cross-bedded, white, or reddish sandstones with scarce marly and carbonate intercalations. The presence of this unit involves a significant basinward coastal shift. Its age ranges from the latest Kimmeridgian to the latest Tithonian or even to the earliest Berriasian (Aurell et al., 2019).

Middle-Upper Triassic Germanic-type facies of coastal and shallow-marine environments, such as Muschelkalk and Keuper facies, have been mapped in the Camarena de la Sierra outcrops. Muschelkalk facies consist of carbonate deposits, mainly dolostones, and breccias formed by evaporite dissolution. Keuper facies are composed of versicolor clays and marls, salt, and gypsum.

Covering Neogene–Quaternary detrital sediments (conglomerates, sands, clays, and breccias) have been mapped in the Sarrión, La Puebla de Valverde, and Camarena de la Sierra outcrops.

The sedimentary cycles affecting the aforementioned lithostratigraphic units and volcanic levels include the second-order (LJ-2, LJ-3, LJ-4, and MJ-1) and the third-order (LJ2-2, LJ3-1, LJ3-2, LJ3-3, LJ4-1, and LJ4-2) transgressive-regressive facies cycles defined by Gómez et al. (2004) and Gómez & Goy (2005). The spatio-temporal relationships between the lithostratigraphic units and their correlation with the Lower and Middle Jurassic transgressive-regressive facies cycles are illustrated in the synthetic chronostratigraphic chart of Fig. 4.

### Quantifying and dating the volcanic levels

Thirteen successive volcanic levels were identified and accurately dated in all or most of the sites where they crop out, as the relative age of carbonate strata immediately below and above each volcanic level could be estimated by biostratigraphic methods, in most cases at the ammonite zone or even subzone scale. From oldest to youngest, their ages are as follows:  $V_1$  (early Pliensbachian, *jamesoni* Zone or later),  $V_2$  (late Pliensbachian),  $V_3$  (late Pliensbachian, *spinatum* Zone),  $V_4$  (late Pliensbachian, uppermost *spinatum* Zone),  $V_5$  (early Toarcian, *serpentinum* Zone, *elegantulum* Subzone),  $V_6$  (early Toarcian, *serpentinum* Zone, uppermost *elegantulum* Subzone or lowermost *falciferum* Subzone),  $V_7$  (early Toarcian, *bifrons* Zone, *sublevisoni* Subzone),  $V_8$  (early Toarcian, *bifrons* Zone, *bifrons* Subzone),  $V_9$  (late Toarcian, *variabilis* Zone),  $V_{10}$  (late Toarcian, *thouarsense* Zone),  $V_{11}$  (Aalenian, *murchisonae* Zone),  $V_{12}$  (Aalenian *concavum*-Bajocian *discites* zonal boundary),  $V_{13}$  (early Bajocian, uppermost *laeviuscula* Zone or *laeviuscula-propinquans* zonal boundary), according to Cortés (2018, 2020a, 2021) (Fig. 5).

The oldest volcanic record of the SE Iberian Range had always been considered to be included in the Barahona Formation (e.g., Ortí & Vaquer, 1980; Martínez et al., 1996, 1997, 1998; Martínez-González et al., 1996; Gómez et al., 2004; Lago et al., 2004; Gómez & Goy, 2005). The papers by Cortés & Gómez (2016, 2018) or Cortés (2018, 2020a) made it known that there is an even older volcanic level within the Cuevas Labradas Formation: the early Pliensbachian (*jamesoni* Zone or later) in age volcanic level  $V_1$  (Fig. 5).

### Nature and age of the volcanism

The Jurassic volcanism of the Iberian Range is represented by basaltic rocks with chemical alkaline affinity (Ancochea et al., 1988; Lago et al., 2004). Three types of volcanic deposits can be distinguished:

- 1) Lava flows, which are composed of olivine, augite, variable proportions of plagioclase (Ancochea et

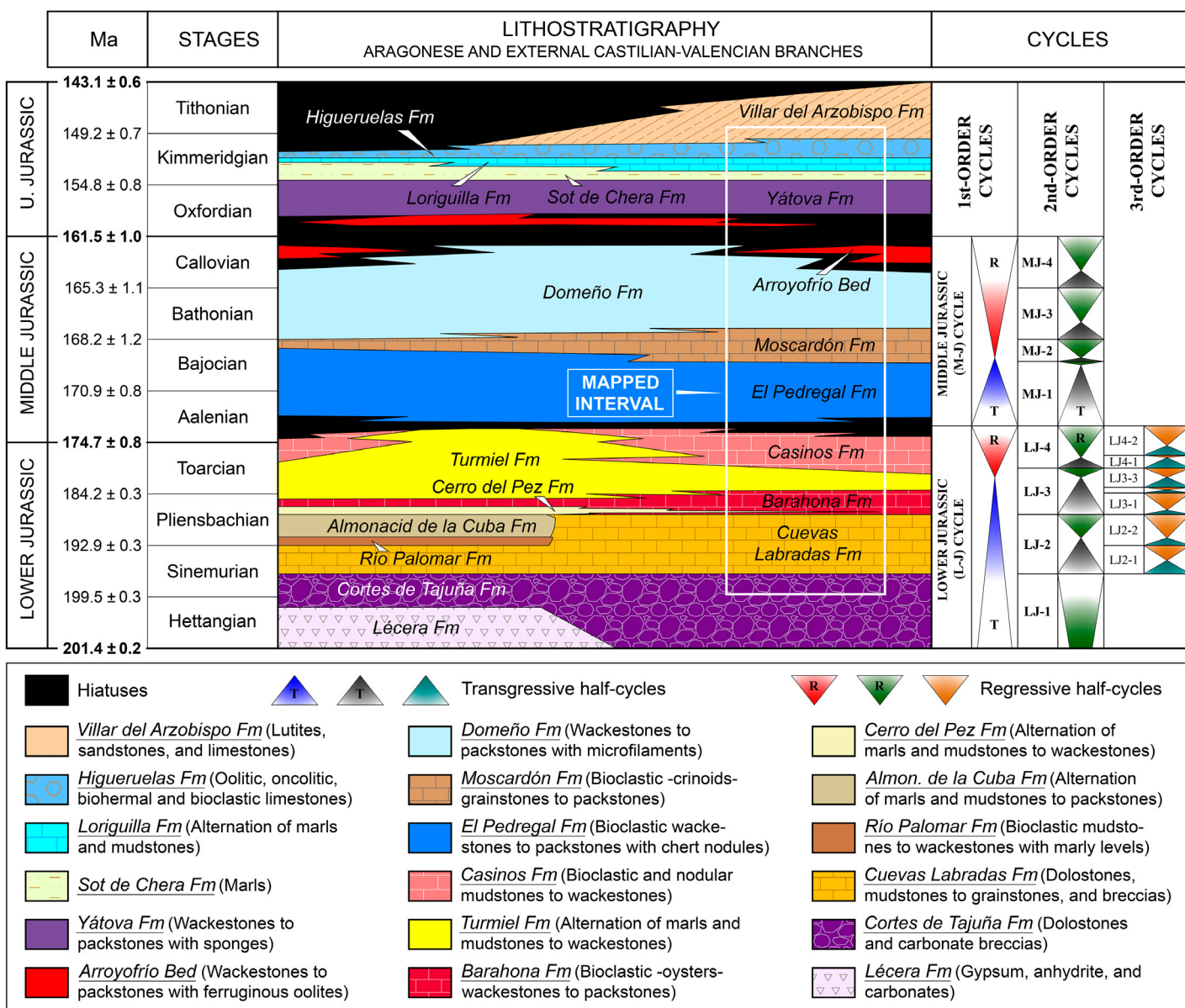


Fig. 4 - Synthetic chronostratigraphic chart showing the Lower and Middle Jurassic lithostratigraphic units and the sedimentary cyclicity across the Aragonese and Castilian-Valencian branches of the Iberian Range (adapted from Gómez et al., 2004 and Aurell et al., 2019). The time scale used is that of Cohen et al. (2013 updated) "International Chronostratigraphic Chart (2024)".

al., 1988; Lago et al., 2004), and abundant vesicles filled with calcite. Although lava flows are scarce, they have been detected in the outcrops of Caudiel (volcanic levels  $V_4$  and  $V_{12}$ ), Sarrión.1 and Sarrión.2 (volcanic level  $V_{12}$ ), La Puebla de Valverde.2 and La Puebla de Valverde.3 (volcanic level  $V_8$ ), and La Puebla de Valverde.4 (volcanic level  $V_6$ ) (Cortés, 2023) (Fig. 5). Pillow lavas have been found in the outcrops of Caudiel (volcanic level  $V_{12}$ ) (Fig. 6A) and La Puebla de Valverde.3 (volcanic level  $V_8$ ) (Fig. 6B).

2) Primary volcaniclastic deposits are constituted of fragmentary material originating from explosive pyroclastic mechanisms. Fragmentary material

includes juvenile fragments of magma cooled before primary accumulation, as well as accidental fragments derived from the pre-volcanic sediments.

3) Secondary volcaniclastic, or epiclastic, deposits are primary volcaniclastic deposits that have been modelled by sedimentary environment agents, such as currents, waves, tides, or storms, after their primary accumulation.

Primary volcaniclastic deposits (pyroclastic) of any volcanic level grade laterally into secondary volcaniclastic deposits (epiclastic). Therefore, pyroclastic and epiclastic deposits can be found in almost all volcanic levels (Cortés, 2016, 2020b, 2023).

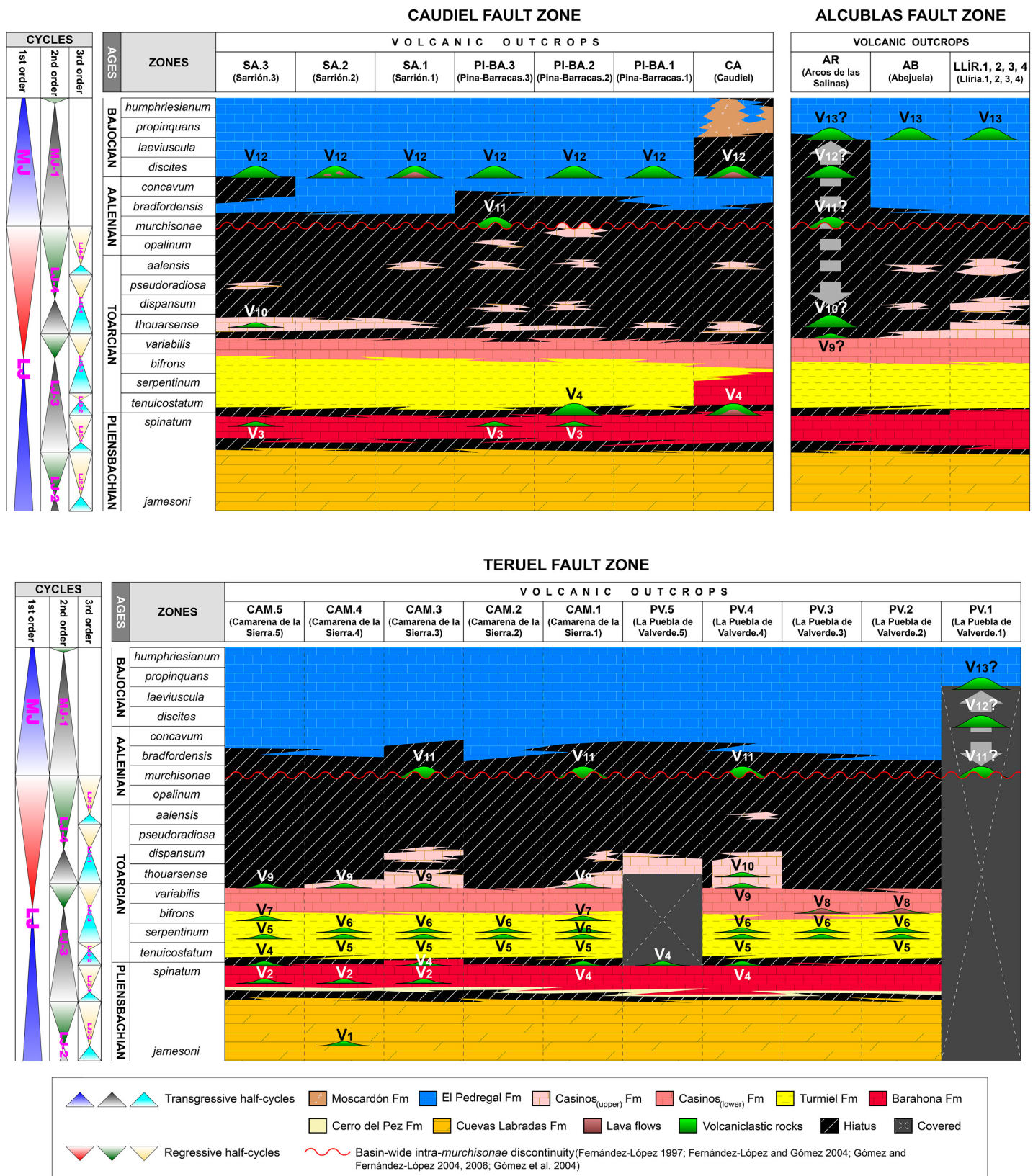


Fig. 5 - Temporal distribution of volcanic levels along the Caudiel, Alcublas and Teruel fault zones. Due to a sedimentary gap from late Toarcian to early-middle Bajocian in the Arcos de las Salinas outcrop (Alcublas Fault Zone), the volcanic level could be  $V_9$ ,  $V_{10}$ ,  $V_{11}$ ,  $V_{12}$ , or even  $V_{13}$ .

The pre-volcanic sediments are covered in some outcrops, and such circumstance prevents determining whether the volcanic level is V<sub>1</sub>–V<sub>2</sub> or V<sub>3</sub> in the La Puebla de Valverde 1 outcrop.

The marly Cerro del Pez Formation has a negligible thickness in the outcrops of the Caudiel and Alcublas fault zones, so it has been included in the Barahona Formation.



Fig. 6 - Pillow lavas A) in the Caudiel outcrop (volcanic level  $V_{12}$ ), currently visible due to recent dismantling for the expansion of the road CV-203, B) in the La Puebla de Valverde.3 outcrop (volcanic level  $V_8$ ). Hammer is 27 cm long.

Except for the scattered lava flows mentioned above, the 13 volcanic levels are mainly of a detrital volcaniclastic nature. Moreover, they were deposited in often shallow or very shallow marine environments, so they were most likely subjected to the action of storm waves and occasionally to fair-weather waves. Such conditions could lead to the remobilisation of these deposits, which could then be partially or totally redeposited on younger substrates than those on which they initially accumulated.

Cortés (2023) described a series of criteria to differentiate primary volcaniclastic deposits and applied them to the volcanic levels of all outcrops in the SE of the Iberian Range. Only three volcanic levels ( $V_1$ ,  $V_7$ , and  $V_{10}$ ) show neither lava flows nor primary volcanic deposits, but rather a mixture of volcanic and sedimentary components, often with tractional sedimentary structures, invertebrate marine fossils, and bioturbation. These three volcanic levels could be portions derived from volcanic edifices preserved in the subsurface or already entirely eroded, and they could be coeval or more recent than the volcanism age (Cortés, 2023). The conclusion is that the ages of the stratigraphic emplacement of at least 10 of the 13 volcanic deposits are representative of volcanic events. Since the youngest volcanic level ( $V_{13}$ ) is a genuine primary volcanic deposit (Cortés, 2023), the early Pliensbachian–early Bajocian interval is a period during which magmatic manifestations were recorded in the westernmost margin of the Tethys. Moreover, as the volcanic level  $V_1$  could not be coeval with the volcanic event that originated it, but more recent, the lower age of the interval could also be slightly older.

### Volcanism during the first Mesozoic post-rifting stage of the Iberian Basin

Despite the expected tectonic and volcanic quiescence during a post-rifting stage, Gómez (1979), later supported by the works of Fernández-López & Gómez (2004) and Gómez & Goy (2005), reported the existence of a network of NW and NE trending synsedimentary faults affecting the eastern part of Iberia and delimiting depocentres and topographic highs. Gómez (1979) realised that the outcrops of volcanic rocks align along three fault zones: the NW–SE Caudiel and Alcublas fault zones and the NE–SW or NNE–SSW trending Teruel Fault Zone.

It is of great interest that Van Wees et al. (1998) detected the existence of a period of rapid tectonic subsidence during the Pliensbachian–Toarcian interval in the Iberian Basin. Thus, this time span is embedded within the first post-rifting stage established by Gómez et al. (2004, 2019) and characterised by thermal subsidence. Much of the fault-controlled volcanism falls inside this lapse of tectonic subsidence proposed by Van Wees et al. (1998).

## METHODS AND TECHNIQUES

### Fieldwork

The research was primarily based on fieldwork during different campaigns developed in the first decade of the 2000s. The volcanic levels and adjacent sediments were traditionally mapped (about 100 km<sup>2</sup>) on topographic maps available in paper format at a scale of 1:25,000 provided by the Instituto Geográfico Nacional (IGN) of Spain and at a scale of 1:10,000 by the Institut Cartogràfic Valencià. To achieve this goal, it was essential to carry out a previous exploration of the region to locate all the areas with outcropping volcanic rocks, as well as to recognise the lithostratigraphic units defined by Goy et al. (1976), Gómez et al. (2003), and Gómez & Fernández-López (2004).

### Field mapping digitising process

In this work, georeferenced and three-dimensional sheets of the National Topographic Base [Base Topográfica Nacional (BTN)] at the scale of 1:25,000 (Datum ETRS89 compatible with WGS84, projection UTM, zone 30, and with a curve equidistance of 10 m) in .dwg format have been used as a topographic base for the maps. The z-axis elevations have been set to 0, and much of the original sheet content has been removed because it was deemed irrelevant for this purpose.

The IGN website also offers the possibility to download georeferenced orthoimages in various formats and scales. One of them is “Orthophotos PNOA (Plan Nacional de Ortofotografía Aérea) maximum updating”, at a scale of 1:25,000, in georeferenced tagged image file format (.geotiff), with a resolution of 0.25 m. However, in this work, it has been used the “Orthophotos SIGPAC (Sistema de Información Geográfica de Parcelas Agrícolas) (1997–2003)”, at scale 1:50,000, in enhanced compression wavelet format (.ecw), since many of the mapped areas are located between several sheets of scale 1:25,000 and the 1:50,000 orthoimage mosaics still maintain a good image resolution (0.25–1 m). In addition, it was the orthophoto mosaic that was available when field mapping began in the early 2000s.

Both versions are presented in the geodetic reference system ETRS89, UTM projection, and can be opened within AutoCAD software.

The Digital Elevation Models (DEM) [Modelos Digitales del Terreno (MDT)] are also available on the IGN page. For this work, the “MDT02, second coverage (2015–present)” with a 2 m cell size, at a scale of 1:25,000, in .geotiff format has been downloaded. The digital elevation models have not been used directly in the preparation of the geological maps but have been transformed into shadow maps (.tiff format) to give a perception of relief using the ArcGIS toolbox.

Digital topography, digital elevation models, shadow maps and orthophotos have been spatially handled using ArcGIS software. They formed the basis on which all the other components of the geological mapping (digitised faults, contacts, both between formations and between these and volcanic levels, strikes and dips of beds and all kinds of field notes) were superimposed to form the 2D geological maps within the AutoCAD interface.

To match the topographic base, orthophotos and DEMs/Hillshades at the same scale in both AutoCAD and ArcGIS, the scale of the BTN sheets has been maintained. Although each BTN sheet represents the surface of a 1:25,000 sheet, the viewing scale at which they are downloaded is 1:1000. That is, 1000 drawing units (mm, as AutoCAD is configured in mm) are equivalent to 1000 terrain units (m). In this way, the UTM grid, spaced at 1000 m intervals, can be easily established, and any point can be georeferenced straight away. This scale has served as a working benchmark for the elaboration of the geological maps. Finally, to fit them in an A3 or A2 size, they have been resized to the most convenient scale.

The ArcGIS software allows the import of AutoCAD dwg files. Once those are converted into .shp files, ArcGIS works with 2D components in its ArcMAP version and 3D renderings in its ArcSCENE one. Moreover, ArcGIS can also transform .shp files into .kmz files, compatible with the Google Earth application. Thus, some regions of the 2D maps have also been three-dimensionally displayed (both from ArcSCENE and Google Earth).

As the presentation is required in .pdf format and AutoCAD does not provide a proper transformation due to the complexity and large size of the maps, the final result has been produced using Adobe Illustrator vector processing software. AutoCAD vectorial dwg files are compatible and can be opened in Illustrator, although the editing work required afterwards has not been minor.

The figures included in the paper text have been processed following the same treatment (drawn directly in AutoCAD and utilising Adobe Illustrator to obtain files in .pdf format) and then converted to a raster format (.tiff, .png, or .jpg) and edited using Adobe Photoshop.

## CONTENTS DESCRIPTION

### Criteria used to name the volcanic outcrops

Along the three most relevant tectonic elements (fault zones), eight volcanic sites have been identified, each of which may record a single or several volcanic outcrops. The volcanic sites have been arranged in this way: 1) volcanic sites aligned within the Caudiel Fault Zone, 2) volcanic sites aligned within the Alcublas Fault Zone, and 3) volcanic sites

aligned within the Teruel Fault Zone, the names of the sites being taken from the name of the municipal district in which they are included, either totally or mostly. The acronyms of the volcanic sites in the Caudiel Fault Zone are as follows: CA (CAUDIEL), PI-BA (PINA DE MONTALGRAO-BARRACAS), and SA (SARRIÓN). The acronyms of the volcanic sites in the Alcublas Fault Zone are LLÍR (LLÍRIA), AB (ABEJUELA), and AR (ARCOS DE LAS SALINAS). The acronym of each volcanic outcrop will be followed by an order number from east to west when there is more than one in each site (e.g., SA.1, PI-BA.2, etc.) (Fig. 1).

However, this criterion is not operative to the outcrops aligned within the Teruel Fault Zone due to the large number of them (in many of which the names of the same municipal districts coincide) or to their great extent (sometimes occupying part of several bordering municipal districts). To simplify, they have been denominated in this way: PV (LA PUEBLA DE VALVERDE), those located on the La Puebla de Valverde sheet (E. 1:50,000), and CAM (CAMARENA DE LA SIERRA), those included in the Camarena de la Sierra sheet (E. 1:50,000). The acronyms of the outcrops in the LA PUEBLA DE VALVERDE and CAMARENA DE LA SIERRA sites will be followed by an order number, starting from east to west and north to south (Fig. 1).

### Maps number, dimensions, and content

This paper presents eight geological maps corresponding to the eight volcanic sites, which are distributed in this way (see also Fig. 1):

#### *Caudiel Fault Zone (from SE to NW)*

- 1) CAUDIEL site: Map of the Caudiel outcrop (CA) [volcanic levels  $V_4$  and  $V_{12}$ ]
- 2) PINA-BARRACAS site: Map of the Pina-Barracas outcrops (PI-BA.1, PI-BA.2, and PI-BA.3) [volcanic levels  $V_3$ ,  $V_4$ ,  $V_{11}$ , and  $V_{12}$ ]
- 3) SARRIÓN site: Map of the Sarrión outcrops (SA.1, SA.2, and SA.3) [volcanic levels  $V_3$ ,  $V_{10}$ , and  $V_{12}$ ]

#### *Alcublas Fault Zone (from SE to NW)*

- 4) LLÍRIA site: Map of the Lliria outcrops (LLÍR.1, LLÍR.2, LLÍR.3, and LLÍR.4) [volcanic level  $V_{13}$ ]
- 5) ABEJUELA site: Map of the Abejuela outcrop (AB) [volcanic level  $V_{13}$ ]
- 6) ARCOS DE LAS SALINAS site: Map of the Arcos de las Salinas outcrop (AR) [only one volcanic level crops out and could correspond both to  $V_9$  and  $V_{10}$ ,  $V_{11}$ ,  $V_{12}$ , or  $V_{13}$  (see the explanation in the attached map and Fig. 5)]

#### *Teruel Fault Zone (from N to S)*

- 7) LA PUEBLA DE VALVERDE site: Map of the La Puebla de Valverde outcrops (PV.1, PV.2, PV.3, PV.4, and

PV.5) [volcanic levels  $V_4$ ,  $V_5$ ,  $V_6$ ,  $V_8$ ,  $V_9$ ,  $V_{10}$ ,  $V_{11}$ , and  $V_{12}$  or  $V_{13}$ ]

8) CAMARENA DE LA SIERRA site: Map of the Camarena de la Sierra outcrops (CAM.1, CAM.2, CAM.3, CAM.4, and CAM.5) [volcanic levels  $V_1$ ,  $V_2$ ,  $V_4$ ,  $V_5$ ,  $V_6$ ,  $V_7$ ,  $V_9$ , and  $V_{11}$ ]

The maps were created in .dwg format and finally transformed into the requested .pdf format using Adobe Illustrator. Each of the smaller maps, with a single outcrop (i.e., Caudiel, Abejuela, and Arcos de las Salinas outcrops), has been included in a work table of A3 size at a numerical scale of 1:25,000. The geological maps of the Sarrión outcrops have also been drawn on an A3-size sheet, but at a scale of 1:50,000. The Pina-Barracas, Llíria, and La Puebla de Valverde outcrops have been mapped on A2-size sheets at a numerical scale of 1:50,000. Finally, the outcrops of Camarena de la Sierra fit on an A3 sheet at a numerical scale of 1:100,000. Each map contains a main 2D geological cartography, whose legend includes a brief description of the lithostratigraphic units that encompass the volcanic levels. At least one location map always goes with the 2D mapping and shows its positioning within the corresponding volcanic alignment and topographic/geological sheet (1:50,000). In single-outcropped volcanic sites, where the topographic base is restricted to the cartographic boundaries (i.e., Caudiel, Abejuela, and Arcos de las Salinas outcrops), a second additional location map has been included. It shows the geographical situation of the 2D mapped area within the corresponding topographic base of the sheet 1:25,000. Additionally, 3D mappings are displayed of some interesting partial areas of the main 2D map (Caudiel, Llíria, Abejuela, and Arcos de las Salinas outcrops). These 3D maps have been obtained from ArcSCENE (ArcGIS) and Google Earth. To emphasise the relief, clipped shadow maps have been used to overlay the 2D cartography and also the 3D mapping obtained with ArcSCENE. Hillshade maps have also been placed under the location maps, giving a virtual three-dimensional effect. Clipped orthophotos have been incorporated into the miniature location maps of the 3D mappings from Google Earth (Caudiel, Llíria, Abejuela, and Arcos de las Salinas outcrops). Partial orthophoto clippings have also been implemented, with only the mapping of outcropping volcanic rocks superimposed on them (Pina-Barracas outcrops). Stratigraphic cross-sections have also been introduced in some maps (Caudiel outcrop), as well as chronostratigraphic descriptions and diagrams to explain certain peculiarities (Arcos de las Salinas outcrop).

The Order FOM/2807/2015 of 18 December 2015, issued by the Ministerio de Fomento de España, states in Article 4 that the use of the digital geographic data products of the Instituto Geográfico Nacional will be free and open when provided that the origin and ownership of the data

is mentioned under the corresponding licence for use. The access and utilisation of these products imply acceptance of a CC-BY 4.0 licence. When the user modifies the original product and thus generates a new one, the following must be mentioned: "work derived from BTN CC-BY 4.0 ign.es." for clipped BTN sheets (2D maps), "work derived from Orto-SIGPAC 1997-2003 CC-BY 4.0 scne.es." for clipped orthoimages, and "work derived from MDT02-cob2 2015-2021 CC-BY 4.0 scne.es." for clipped DEMs/Hillshades. These indications have been stated in the legends of the corresponding maps.

## DISCUSSION AND CONCLUSIONS

When looking at the 2D arrangement of the outcrops, one would think that some outcrops could have been grouped into a single one due to their proximity (as is the case of CAM.4, which could have been included within CAM.5, or even have merged the CAM.1, 3, 4, and 5 outcrops into a single super outcrop). However, the areas specially covered by debris or vegetation that separate them have prevented the lateral tracking of the lithostratigraphic units and volcanic levels and have determined that they were kept as independent outcrops.

On the other hand, some volcanic levels extend beyond the cartographic limits. However, in most cases, these volcanic levels are close to their lateral wedging and disappearance, showing a reduced thickness. Their characterization, identification and dating have been sufficiently contrasted within the cartographic limits.

Regarding the cartographic units of the maps, which generally coincide with the rank of "formation" (lithostratigraphic unit), a few considerations could be made:

- 1) According to Gómez (1979) and Cortés (2018), the marly Cerro del Pez Formation, recorded between the Cuevas Labradas and Barahona formations (Fig. 4), had not been deposited in the southeastern sector of the Castilian-Valencian Branch (Fig. 1), which includes the southern and eastern parts of the studied area. However, in the northwestern part of the studied area (Javalambre and Camarena ridges in the Teruel Fault Zone), intervals of marls and marlstones of up to 2-4 m thick are interspersed in the basal part of the Barahona Formation. These marly intervals could be viewed as belonging to the Cerro del Pez Formation, as stated in the IGME geological map memory of La Puebla de Valverde (Adrover et al., 1983). Therefore, the Cerro del Pez Formation has been mapped in the outcrops of La Puebla de Valverde and Camarena de la Sierra. In contrast, marly intervals less than 2m thick

observed in the southeasternmost outcrops have not been mapped due to scale reasons.

2) The Middle Jurassic El Pedregal, Moscardón, and Domeño formations have been grouped into a single cartographic unit called “Ped-Mos-Dom”, noting that the latest and youngest volcanic bodies are included only in the El Pedregal Formation, not in the Moscardón or Domeño formations. The exception is the Caudiel outcrop, where the three Middle Jurassic formations onlap the flanks of the most significant volcanic mound (Gómez, 1979; Cortés & Gómez, 2016; Cortés, 2018, 2020b, 2021, 2023). Therefore, it has been preferred to map them independently. The intricate relationships between these three formations, especially those of El Pedregal and Moscardón, in the Caudiel outcrop, are outlined in Cortés (2020b). The presence of positive seafloor reliefs (the volcanic mound) and locally active syn-sedimentary tectonics conditions their contacts. For example, the El Pedregal Formation shifts laterally and upwards to the Moscardón Formation, even downwards on the flanks of the mound (Cortés, 2020b).

3) The Casinos Formation shows two well-differentiated lithofacies: a lower one constituted by nodular limestones (mudstone-wackestone) of bluish-grey tones and an upper one of very nodular and bioclastic wackestones-packstones of yellowish-brown tones. The volcanic level  $V_9$  (*variabilis* Zone in age), present only in the La Puebla de Valverde and Camarena de la Sierra outcrops, accumulated on top of the lower part of the Casinos Formation and generated a positive relief, occupying accommodation space and partially preventing the deposition of the upper part of the Casinos Formation. In determined sectors of the La Puebla de Valverde and Camarena de la Sierra outcrops, the upper part of the Casinos Formation is absent, regardless of whether the volcanic level  $V_9$  was deposited. Two cartographic units have been distinguished within the Casinos Formation to reflect this circumstance: the lower infravolcanic one referred to as “Cas<sub>(lower)</sub>” and the upper supravolcanic one called “Cas<sub>(upper)</sub>”, in the La Puebla de Valverde and Camarena de la Sierra geological maps. In the remaining outcrops, the cartographic unit “Cas” includes the lower and upper parts of the Casinos Formation.

As for the colours used, they have been kept the same on all 2D and 3D maps. However, they do not conform to the colours recommended by international codes and commissions. Both the “International Stratigraphic Chart (IUGS)” and the “Colour Code according to the Commission for the Geological Map of the World (CGMW)”, make recommendations for the use of colour in “stages”. In this work, much more detailed mapping is being done. The mapping units are formations or layers, with several mapping/lithostratigraphic units generally mapped within each stage. Following the criteria of these commissions, the colouring of units would result in a gradation of blue tonalities that would be practically indistinguishable, especially if their opacity has to be reduced by overlaying them with shadow maps or Google Earth photos. It has been preferred to maintain bright colours that are highly contrasted with each other (e.g., alternating light and dark colours).

In conclusion, a set of outcrops of volcanic rocks has been detected distributed along eight volcanic sites in the SE Iberian Range. On the outcrop as a whole, thirteen volcanic levels of different ages have been identified and dated by biostratigraphic methods, of which at least ten have been identified as primary pyroclastic deposits, leaving open the question of whether the epiclastic levels  $V_1$ ,  $V_7$ , and  $V_{10}$  represent the products of volcanic events or, on the contrary, are remobilisations of other primary volcanic levels redeposited on more modern substrates. These magmatic manifestations have been plotted on the maps presented in this work and represent the overall Jurassic magmatism of the entire Iberian Range. The geological maps could be of great interest as a reference and starting point for further studies in different geological disciplines.

## ACKNOWLEDGMENTS

Firstly, I recognise the relevance of the Geological Field Trips and Maps journal’s aim and scope. The author thanks the Editor-in-Chief, Marco Malusà, and the Associate Editor, Guido Giordano, for handling this work. The Editor Manager, Fabio Massimo Petti, is thanked for his indications, advice, and guidance. I am also grateful to Associate Editor Guido Giordano, an anonymous reviewer, and the Editor Manager of the Geological Survey of Italy, Angelo Cipriani, for their helpful comments and suggestions, which significantly improved the manuscript and maps. I cannot but thank the Instituto Geográfico Nacional of Spain for their significant data contributions and availability for free download on their outstanding website.

## REFERENCES

Abril J., García F., González F., Iglesias M., Ortí F. & Rubio J. (1975) - Mapa Geológico de España 1:50,000 (2nd series), Sheet No. 638 (Alpuente). IGME, Madrid.

Abril J., Apalategui O., Ferreiro E., García F., González F., Hernández E., Lago E., Ortí F., Pliego D.V., Quintero I. & Rubio J. (1978) - Mapa Geológico de España 1:50,000 (2nd series), Sheet No. 613 (Camarena de la Sierra). IGME, Madrid.

Adrover R., Aguilar M.J., Alberdi M.T., Aragón E., Aznar J.M., Comas M.J., Gabaldón V., Giner J., Godoy A., Goy A., Gutiérrez M., Leal M.C., Moissenet E., Olivé A., Portero J.M., Ramírez J.I. & Ramírez del Pozo J. (1983) - Mapa Geológico de España 1:50,000 (2nd series), Sheet No. 590 (La Puebla de Valverde). IGME, Madrid.

Ancochea E., Muñoz M. & Sagredo J. (1988) - Identificación geoquímica del vulcanismo Jurásico de la Cordillera Ibérica. *Geociencias* (Aveiro), 3(1-2), 15-22.

Aurell M., Fregenal-Martínez M., Bádenas B., Muñoz-García M.B., Élez J., Meléndez N. & de Santisteban C. (2019) - Middle Jurassic-Early Cretaceous tectono-sedimentary evolution of the southwestern Iberian Basin (central Spain): Major palaeogeographical changes in the geotectonic framework of the Western Tethys. *Earth-Sci. Rev.*, 199, 102983, <https://doi.org/10.1016/j.earscirev.2019.102983>.

Bakx L.A.J. (1935) - La géologie de Cascante del Río et de Valacloche (Espagne). *Leid. Geol. Meded.*, 7(2), 157-220.

Blakey R. (2011) - Paleogeography of Europe Series. Deep Time Maps. Retrieved in June 2022, from <https://www.deeptimemaps.com/map-room/>.

Campos C., González F., Goy A., Lazuen J., Martín P. & Ortí F. (1977) - Mapa Geológico de España 1:50,000 (2nd series), Sheet No. 639 (Jérica). IGME, Madrid.

Cohen K.M., Finney S.C., Gibbard P.L. & Fan J.-X. (2013; updated) - The ICS International Chronostratigraphic Chart. *Episodes*, 36(3), 199-204. <https://stratigraphy.org/chart>

Cortés J.E. (2018) - La arquitectura deposicional de los carbonatos del Jurásico Inferior y Medio relacionados con los materiales volcánicos del sureste de la Cordillera Ibérica. PhD thesis, Universidad Complutense, Madrid. <https://eprints.ucm.es/id/eprint/56088/>

Cortés J.E. (2020a) - Volcanic rocks in Lower Jurassic marine carbonate successions in the southeastern Iberian Range (Spain): biochronostratigraphic dating. *J. Iber. Geol.*, 46(3), 253-277, <https://doi.org/10.1007/s41513-020-00134-z>.

Cortés J.E. (2020b) - Interaction between volcanism, tectonics and sedimentation in a shallow carbonate platform: A case study from the western Tethys (Middle Jurassic, southeastern Iberian Range). *Estud. Geol.-Madrid*, 76(1), e129, <https://doi.org/10.3989/egeol.43590.537>.

Cortés J.E. (2021) - Using high-resolution ammonite biochronostratigraphy to date volcanicogenic deposits preserved in Middle Jurassic carbonate platforms successions of the westernmost Tethys (southeastern Iberian Range, Spain). *Riv. Ital. Paleontol. S.*, 127(3), 557-583, <https://doi.org/10.13130/2039-4942/16364>.

Cortés J.E. (2023) - Dating volcanic materials through biochronostratigraphic methods applied to hosting strata (example from the Iberian Chain, eastern Spain). *CR. Géosci.*, 355, 175-201, <https://doi.org/10.5802/crgeos.220>.

Cortés J.E. & Gómez J.J. (2016) - Middle Jurassic volcanism in a magmatic-rich passive margin linked to the Caudiel Fault Zone (Iberian Range, East of Spain): biostratigraphical dating. *J. Iber. Geol.*, 42(3), 335,354, <https://doi.org/10.5209/JIGE.54667>.

Cortés J.E. & Gómez J.J. (2018) - The epiclastic barrier-island system of the Early-Middle Jurassic in eastern Spain. *J. Iber. Geol.*, 44(2), 257-271, <https://doi.org/10.1007/s41513-018-0061-7>.

Fernández-López S. (1997) - Ammonites, taphonomic cycles and stratigraphic cycles in carbonate epicontinental platforms. *Cuad. Geol. Ibér.*, 23, 95-136.

Fernández-López S. & Gómez J.J. (2004) - The Middle Jurassic Eastern margin of the Iberian platform system (eastern Spain). Palaeogeography and biodispersal routes of ammonoids. *Riv. Ital. Paleontol. S.*, 110(1), 151-162, <https://doi.org/10.13130/2039-4942/6281>.

Gautier F. (1968) - Sur l'existence et l'age d'un paléovolcanisme dans le Jurassique sud-aramonais (Espagne). *C. R. Somm. Séances Soc. Géol. Fr.*, 3, 74-75.

Gautier F. (1974) - Mapa Geológico de España 1:50,000 (2nd series), Sheet No. 614 (Manzanera). IGME, Madrid.

Gautier F. & Odin G.S. (1985) - Volcanisme Jurassique du sud de l'Aragon (Espagne). *Bulletin de Liaison et Information, I.G.C.P. Project 196*, offset Paris, 5, 34-38.

Gómez J.J. (1979) - El Jurásico en facies carbonatadas del sector levantino de la Cordillera Ibérica. *Seminarios de Estratigrafía, Serie Monografías 4*. Universidad Complutense de Madrid-Consejo Superior de Investigaciones Científicas, Madrid.

Gómez J.J. & Fernández-López S. (2004) - Las unidades litoestratigráficas del Jurásico Medio de la Cordillera Ibérica. *Geogaceta*, 35, 91-94.

Gómez J.J. & Fernández-López S.R. (2006) - The Iberian Middle Jurassic carbonate-platform system: synthesis of the palaeogeographic elements of its eastern margin (Spain). *Palaeogeogr. Palaeocl.*, 236(3-4), 190-205. <https://doi.org/10.1016/j.palaeo.2005.11.008>

Gómez J.J. & Goy A. (1979) - Las unidades litoestratigráficas del Jurásico medio y superior, en facies carbonatadas del Sector Levantino de la Cordillera Ibérica. *Estud. Geol.-Madrid*, 35, 569-598.

Gómez J.J. & Goy A. (2005) - Late Triassic and Early Jurassic palaeogeographic evolution and depositional cycles of the Western Tethys Iberian platform system (Eastern Spain). *Palaeogeogr. Palaeoclimatol. Palaeoecol.*, 222(1-2), 77-94, <https://doi.org/10.1016/j.palaeo.2005.03.010>.

Gómez J.J., Trell A. & Pérez P. (1976) - Presencia y edad de vulcanitas en el Jurásico del Norte de Valencia (Cordillera Ibérica, España). *Acta Geol. Hisp.*, 1, 1-7.

Gómez J.J., Comas-Rengifo M.J. & Goy A. (2003) - Las unidades litoestratigráficas del Jurásico Inferior de las Cordilleras Ibérica y Costeras Catalanas. *Rev. Soc. Geol. Esp.*, 16(3-4), 227-238.

Gómez J.J., Fernández-López S. & Goy A. (2004) - Primera fase de post-rifting: Jurásico Inferior y Medio. In: Vera, J.A. (Ed), *Geología de España*, 495-503. Sociedad Geológica de España-Instituto Geológico y Minero de España (SGE-IGME), Madrid.

Gómez J.J., Sandoval J., Aguado R., O'Dogherty L. & Osete M.L. (2019) - The Alpine Cycle in eastern Iberia: microplate units and geodynamic stages. In: Quesada C., Oliveira J.T. (Eds), *The Geology of Iberia: A Geodynamic Approach. Volume 3: The Alpine Cycle*, 15-27. Springer Nature, Heidelberg, [https://doi.org/10.1007/978-3-030-11295-0\\_2](https://doi.org/10.1007/978-3-030-11295-0_2).

Goy A., Gómez J.J. & Yébenes A. (1976) - El Jurásico de la rama castellana de la Cordillera Ibérica (Mitad Norte). I. Unidades litoestratigráficas. *Estud. Geol.*-Madrid, 32, 391-423.

Lago M., Arranz E., Gil A. & Pocoví A. (2004) - Magmatismo asociado. In: Vera, J.A. (Ed), *Geología de España*, 522-525. Sociedad Geológica de España-Instituto Geológico y Minero de España (SGE-IGME), Madrid.

Lazuen J. & Roldán R. (1977) - Mapa Geológico de España 1:50,000 (2nd series), Sheet No. 667 (Villar del Arzobispo). IGME, Madrid.

Martin R. (1936) - Die geologie von Camarena de la Sierra und Riodeva (Provinz Teruel, Spanien). *Leid. Geol. Meded.*, 8(1), 55-154.

Martínez R.M., Lago M., Valenzuela J.I., Vaquer R. & Salas R. (1996) - El magmatismo alcalino jurásico del sector SE de la Cadena Ibérica: composición y estructura. *Geogaceta*, 20(7), 1687-1690.

Martínez R.M., Lago M., Valenzuela J.I., Vaquer R., Salas R. & Dumitrescu R. (1997) - El volcanismo Triásico y Jurásico del sector SE de la Cadena Ibérica y su relación con los estadios de rift mesozoicos. *Bol. Geol. Min.*, 108-4 and 5(367-376), 39-48.

Martínez R.M., Vaquer R. & Lago M. (1998) - El volcanismo jurásico de la Sierra de Javalambre (Cadena Ibérica, Teruel). *Teruel*, 86(1), 43-61.

Martínez-González R.M., Lago M., Valenzuela-Ríos J.I. & Arranz E. (1996) - Interés como Patrimonio Geológico de dos magmatismos mesozoicos en la sierra de Javalambre (Teruel). *Geogaceta*, 20(5), 1186-1188.

Odin G.S., Desprairies A., Fullagar P.D., Bellon H., Decarreau A., Fröhlich F. & Zelvelder M. (1988) - Nature and geological significance of celadonite. In: Odin, G.S. (Ed), *Green marine clays. Developments in Sedimentology* 45, 337-398. Elsevier, Amsterdam, [https://doi.org/10.1016/s0070-4571\(08\)70071-2](https://doi.org/10.1016/s0070-4571(08)70071-2).

Ortí F. & Sanfeliu T. (1971) - Estudio del vulcanismo jurásico de Caudiel (Castellón) en relación con procesos de lateritzación, condensación y silificación de la serie calcárea. *Instituto de Investigaciones Geológicas de la Diputación Provincial. Barcelona*, 26, 21-34.

Ortí F. & Vaquer R. (1980) - Volcanismo jurásico del sector valenciano de la Cordillera Ibérica. Distribución y trama estructural. *Acta Geol. Hisp.*, 15(5), 127-130.

Osete M.L., Gómez J.J., Pavón-Carrasco F.J., Villalaín J.J., Palencia-Ortas A., Ruiz-Martínez V.C. & Heller F. (2011) - The evolution of Iberia during the Jurassic from palaeomagnetic data. *Tectonophysics*, 502(1-2), 105-120, <https://doi.org/10.1016/j.tecto.2010.05.025>.

Schettino A. & Turco E. (2011) - Tectonic history of the western Tethys since the Late Triassic. *Geol. Soc. Am. Bull.*, 123(1-2), 89-105, <https://doi.org/10.1130/b30064.1>.

Van Wees J.D., Arche A., Beijendorff C.G., López-Gómez J. & Cloetingh S.A.P.L. (1998) - Temporal and spatial variations in tectonic subsidence in the Iberian Basin (eastern Spain): inferences from automated forward modelling in high-resolution stratigraphy (Permian-Mesozoic). *Tectonophysics*, 300(1-4), 285-310, [https://doi.org/10.1016/s0040-1951\(98\)00244-3](https://doi.org/10.1016/s0040-1951(98)00244-3).

Vergés J., Kullberg J.C., Casas-Sainz A., de Vicente G., Duarte L.V., Fernández M., Gómez J.J., Gómez-Pugnaire M.T., Jabaloy Sánchez A., López-Gómez J., Macchiavelli C., Martín-Algarra A., Martín-Chivelet J., Antón Muñoz J., Quesada C., Terrinha P., Torné M. & Vegas R. (2019) - An introduction to the Alpine Cycle in Iberia. In: Quesada C., Oliveira J.T. (Eds), *The Geology of Iberia: A Geodynamic Approach. Volume 3: The Alpine Cycle*, 1-14. Springer Nature, Heidelberg, [https://doi.org/10.1007/978-3-030-11295-0\\_1](https://doi.org/10.1007/978-3-030-11295-0_1).

*Manuscript received 12 August 2025; accepted 29 December 2025; published online 04 February 2026; editorial responsibility and handling by G. Giordano.*